



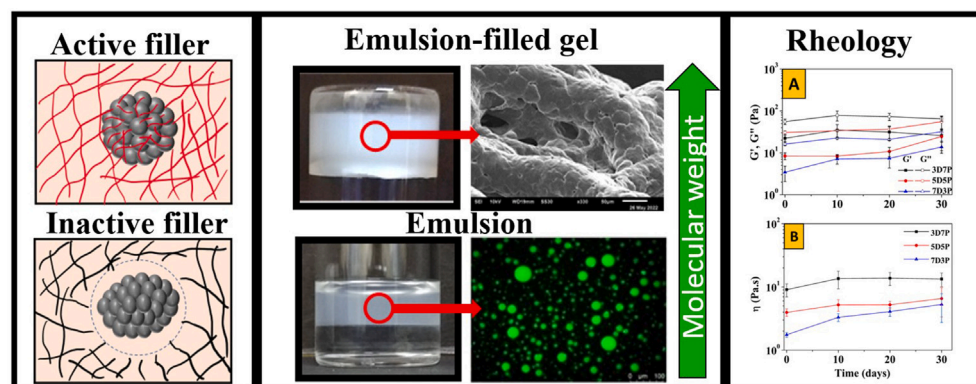
# Probing emulsion-gel transition in aqueous two-phase systems stabilized by charged nanoparticles: A simple pathway to fabricate water-in-water emulsion-filled gels

Chandra Shekhar <sup>a</sup>, Sai Geetha Marapureddy <sup>a</sup>, Vishwajeet Mehandia <sup>a</sup>, Venkateshwar Rao Dugyala <sup>b</sup>, Manigandan Sabapathy <sup>a,\*</sup>

<sup>a</sup> Department of Chemical Engineering, Indian Institute of Technology Ropar, Rupnagar, 140001, Punjab, India

<sup>b</sup> Department of Chemical Engineering, Indian Institute of Science Education and Research, Bhopal, Bhauli, 462066, Madhya Pradesh, India

## GRAPHICAL ABSTRACT



## ARTICLE INFO

**Keywords:**  
W/W emulsions  
ATPS  
Emulsion-filled gels  
Rheology  
Silica nanoparticles

## ABSTRACT

Nanoparticle-stabilized water-in-water (w/w) emulsions, an example of aqueous two-phase systems (ATPS), can produce low-fat food colloids, edible gels, bio-polymer-based bijels, scaffolds for tissue-engineering, and porous materials. This w/w emulsion is made from two thermodynamically incompatible aqueous-polymer solutions, such as polyethylene oxide (PEO) and dextran. Changing the molecular weight of PEO in one aqueous phase stabilizes w/w emulsion. The state diagram we generated using electron and light microscopy provides a novel approach to producing stable emulsion-filled gels and emulsion droplets. The visual examination, brightfield, and fluorescent microscopy studies highlight the role of molecular weight and storage duration. The production of an emulsion-filled gel is ascribed to the “active-filler-particles” arrangement, typically seen when the affinity between droplets stabilized by particles and polymer is substantial. In contrast, we expect the “inactive-filler-particles” arrangement for the samples that undergo phase inversion. The temporal evolution of shear-induced structures recorded using a rheometer demonstrates that these emulsion-filled gels’ viscoelastic properties correspond directly with time, molecular weight, and polymer composition. The emulsion-filled gels generated displayed 90-day storage stability. Our work would help us understand the complex dynamics of w/w emulsion-based formulations that need suitable size, shape, appearance, and shelf life management.

\* Corresponding author.

E-mail address: [mani@iitrpr.ac.in](mailto:mani@iitrpr.ac.in) (M. Sabapathy).

<https://doi.org/10.1016/j.colsurfa.2023.131474>

Received 24 January 2023; Received in revised form 26 March 2023; Accepted 15 April 2023

Available online 25 April 2023

0927-7757/© 2023 Elsevier B.V. All rights reserved.

## 1. Introduction

An emulsion is a mixture of two immiscible liquids in which the droplets of one liquid phase are dispersed into the other. Emulsions are widely available in our daily lives in various households, agrochemicals, cosmetics, and pharmaceutical products. The conventional water-in-oil (w/o) and oil-in-water (o/w) emulsions have been involved in numerous applications, e.g., cosmetics formulation or healthcare and pharmaceutical industries [1]. An extended emulsion system such as an aqueous two-phase system (ATPS) involving polymer–polymer interaction has also been extensively studied from a unique pathway to make porous materials, bijels, and emulsion gels [2]. ATPS is an aqueous binary mixture of two thermodynamically incompatible polymer systems [3]. Water-in-water (w/w) emulsion is a classic example of ATPS, often employed when the oil phase is known to cause harmful effects. For instance, colloidal particles can stabilize w/w emulsions and help address challenges like encapsulating oil-sensitive active ingredients or developing low-fat edible products. These particles, unlike surfactants, can traverse the interfacial boundary, typically a few tens of nanometers thick. However, the water–water interface has unique properties, like an ultra-low interfacial tension of approximately 1  $\mu\text{N/m}$ , making the stabilization process even more complex. To overcome these challenges, one has to devise a suitable strategy to achieve stable emulsions by preventing the destabilization of the dispersed phase due to various instabilities such as coalescence, creaming, and sedimentation due to gravity. Our group reported one such approach to tackle the instabilities earlier using the oppositely charged nanoparticles (OCNPs) by exploiting the interplay between the size and shape of the resulting clusters formed as a result of self-assembly [4]. Alternatively, one can devise an approach in which the droplets are confined within a three-dimensional solid-like aqueous network (hydrogels). In this endeavor, we desired to communicate another exciting avenue in the domain of ATPS, i.e., emulsion-filled gels or emulgels stabilized by the nanoparticles. The rheological properties of these gels depend on the polymer matrix [5]. Stabilizing droplets by inducing the formation of three-dimensional polymer networks can provide insight into the roles of polymers and colloids in pharmaceutical, food, and cosmetic formulations. Furthermore, unlike o/w or w/o Pickering emulsions, the particle-stabilized w/w emulsions offer an extended scope to tune the structure of emulsions, shelf-life, and quality of the products via an additional variability, i.e., the molecular weight of dissolved polymers. This property helps us improve droplets' stability by synergistic stabilization and the formation of polymer bridges between the droplets.

An emulsion-filled gel is a soft solid-like composite material [6–10]. Note: The emulsion-filled gels reported here are different from shake gels which are observed at higher colloidal particle concentration (15–35 wt%), and lower PEO concentration (0.25–0.50 wt%) [11–14]. These emulsion gels can be structurally defined as the emulsion droplets dispersed into the polymeric network-like gel matrix [6]. One of the significant advantages of these complex emulsion systems is the improved stability as the droplets are stabilized by the particles confined within the three-dimensional network of hydrogels. Such an arrangement of polymer gel provides a simple yet straightforward route to stabilize the w/w emulsion using the nanoparticles. That is, the formation of three-dimensional hydrogels promotes the immobilization of droplets within the gel matrix, thereby preventing the early breakdown of droplets due to coalescence. One of the potential applications of the emulsion-filled gels in food formulations is that these structures help produce low-fat food products with improved creaminess perception [15,16]. In the context of particle-stabilized gels, there are two idealized models of structured emulsions, (1) emulsion-filled gels and (2) emulsion gels [17,18]. In the former case, the droplets are immobilized by the three-dimensional network of polymers, while the enhanced stability in the latter is due to the aggregation of the emulsion droplets. For instance, the work demonstrated by *Ayed et al.* represents

the model based on emulsion gels [19]. In that work, using cellulose nanocrystal (CNC) particles in large amounts, i.e., > 1 g/L, results in the formation of bridges between the droplets. One can also use an approach that helps immobilize the droplets via the emulsion-filled gels induced by three-dimensional polymer networks. Here, we demonstrate the stabilization of w/w emulsions via the formation of emulsion-filled gels or gel beads in the matrix of the continuous or dispersed phase. We hypothesize that the type of emulsion decides the resulting structures. For instance, if the polymer that induces the gelation forms the continuous phase, one would get a structure similar to the interconnected bridges exhibiting the three-dimensional porous channels. On the other hand, the change in the emulsion type puts the gelling polymer on the other side, i.e., the dispersed phase, to yield a structure similar to gel beads [20,21]. Here, the stability becomes enhanced through interlocking the particles at the interface. The improved stability could be attributed to the formation of polymer networks in the dispersed phase and adsorption on the surface of particles. Our systematic study helped us explore the role of molecular weight, ageing time, and polymer concentrations in stabilizing w/w emulsion droplets. Further, we employed a rheometer to probe the emulsion-to-gel transition at a particular experimental condition and characterize the rheological properties of emulsion-filled gels. To the best of our knowledge, no studies reported on stabilizing w/w emulsions using the approach proposed by us.

## 2. Experimental

### 2.1. Materials

We used polyethylene oxide (PEO) and dextran, procured from Sigma-Aldrich Chemicals Pvt. Ltd., India, to prepare an ATPS. A known concentration of PEO and dextran labelled with a particular molecular weight (Mwt) was used to prepare an emulsion mixture. To understand molecular weight's influence on the emulsion products' quality, we used PEO with different Mwt. The average molecular weight of PEO employed for the studies were  $1 \times 10^5$  (1E5),  $3 \times 10^5$  (3E5),  $6 \times 10^5$  (6E5), and  $10 \times 10^5$  (10E5) Da, as per the specification of the manufacturer. The average molecular weight of dextran reported by the manufacturer is  $4 \times 10^4$  Da. All the experiments that involve emulsion were carried out by keeping the Mwt of dextran constant while varying the same for PEO. In a few experiments, we used fluorescently-labelled dextran, procured from Sigma-Aldrich Chemical Pvt. Ltd., India, to probe the type of emulsion formed. To stabilize the emulsion, commercially available negatively charged Ludox grade HS-40 (40 wt.%) colloidal suspension containing silica nanoparticles, procured from Sigma-Aldrich Chemicals Pvt. Ltd., India, was used. The average diameter of the HS-40 silica nanoparticles found based on the image analysis using a transmission electron microscope (TEM) was  $16 \pm 2$  nm. An electrophoretic study was carried out to determine the particles' potential at the boundary between the shear and diffuse plane, i.e., Zeta potential ( $\zeta$ ). The  $\zeta$  of the nanoparticles determined for HS-40 in 1 mM NaCl electrolyte medium was  $-55 \pm 1.8$  mV. We used deionized water (18.2 M $\Omega$ ) obtained from a Milli-Q for all experiments.

### 2.2. Preparation of ATPS

To obtain PEO (P) and dextran (D) two-phase mixtures, we used the protocols described elsewhere by our group [4]. In short, we first prepared a different set of an aqueous solution of dextran and PEO in the glass vials and kept them undisturbed overnight after stirring the mixture for 2 min using a vortex shaker. This procedure is required to generate a homogeneous mixture prior to homogenizer-based emulsification. Subsequently, a known concentration of Ludox grade colloidal solution containing silica particles (HS-40) (1 wt% of 2.5 g of the total solution) was added to the dextran solution. Please note the mixing was performed without employing any dispersing agent as

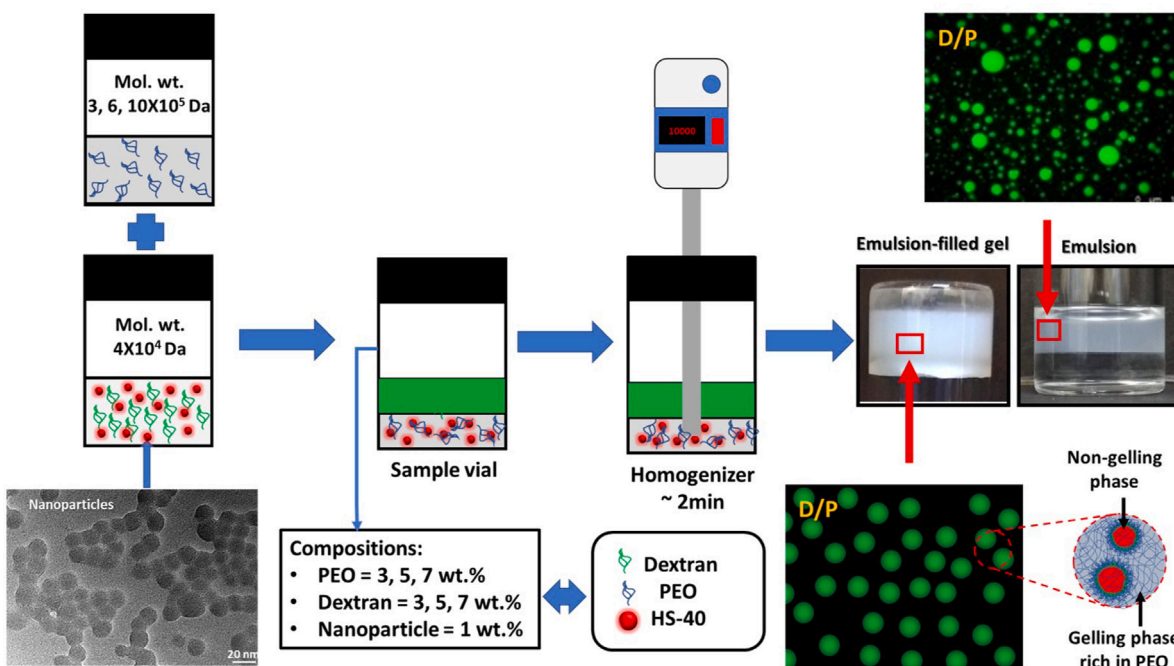


Fig. 1. Schematic description showing the process of making nanoparticle-stabilized w/w emulsions and emulsion-filled gel.

the nature of the HS-40 nanoparticles is hydrophilic, and the contact angle of water with the same found using the sessile drop study is  $14 \pm 1^\circ$ . When added to an aqueous PEO solution, the nanoparticles did not exhibit a preferential orientation effect, since there was no substantial difference in the results. Each vial containing 2.5 g of PEO solution weighing 3, 5, and 7 wt% was combined with aqueous dextran solutions weighing 7, 5, and 3 wt%, respectively, in such a way that the total weight of the solution does not exceed 10 wt%. In every experiment, the nanoparticles concentration in the dextran solution was held constant at 1% by weight. Using a high-pressure homogenizer operating at 10,000 RPM for two minutes, the mixture is emulsified to produce water-in-water emulsion droplets or emulsion-filled gels. Depending on the sample type, these emulsified samples were kept at a constant temperature of 25 °C in an incubator for varying amounts of time. Fig. 1 depicts the schematic explanations of the emulsion-filled gels synthesis procedure. As demonstrated in Fig. 1, the structure of emulsion products can be modified by varying parameters such as molecular weight, composition, and ageing period.

### 2.3. Rheology

The particle-stabilized w/w emulsions and emulsion-filled gels were characterized rheologically using a stress-controlled rheometer with cone-and-plate geometry ( $d = 25$  mm, angle  $2^\circ$ ) equipped with a temperature trap to maintain a constant temperature of 25 °C. Using a spatula, the samples were carefully deposited onto the rheometer plate, and then the upper plate was slowly lowered down towards the sample to minimize structural changes in the samples during loading and handling. For the removal of sample history, these samples were initially sheared at a strain rate of  $0.01$  s<sup>-1</sup>. This method was repeated each time before measurement to get repeatable and geometry-independent data for gel samples, ensuring that our samples lacked wall slip effect and loading history. Each gel sample was subjected to a frequency sweep from  $\omega = 0.1$ –100 rad/s with a continuous oscillatory strain of  $\gamma = 0.1\%$ , followed by an oscillatory strain sweep from  $\gamma = 0.01\%$ –100% at a constant angular frequency  $\omega = 10$  rad/s. During every shear rheological experiment, the storage and loss moduli ( $G'$  and  $G''$ ) were measured. The viscosity of the as-synthesized emulsion products was

measured at a room temperature of 25 °C and a varied shear rate of  $0.01$ – $100$  s<sup>-1</sup>.

All experiments were triplicated to ensure the required consistency of the results. The standard deviation for each data point is within the 5%–10% tolerance limit. We omitted the error bars from certain rheological graphs and displayed the average data from three separate runs. It was done to declutter the information. The creaming index of the as-synthesized emulsion samples was analysed using Image-J software.

### 2.4. Characterization

The electrophoretic study was carried out using the Zeta-sizer (Make: Malvern Panalytical Ltd., Model: Nano ZSP) to measure the  $\zeta$  potential of the HS-40 nanoparticles. We used high-resolution transmission electron microscopy (HRTEM), Make: FEI Company, Model: Tecnai G2 20, to deduce the average size of the HS-40 nanoparticles. To visualize the structural state of APTS in the liquid and solid state, we employed inverted light microscopy (Carl Zeiss. AxioVert. A1) and scanning electron microscopy (SEM), JEOL, JSM-6610. To comment on the type of emulsions, whether PEO-in-dextran (P/D) or dextran-in-PEO (D/P), fluorescent microscopy (Leica Microsystem, DMIL) was used in a few sets of experiments. All the rheological experiments were performed on the MCR-702 rheometer, Anton Paar GmbH, Germany, to characterize the emulsion-filled gels and probe the Pickering emulsion-gel transition. The sessile drop experiments were conducted to determine the three-phase contact angle of water with a suitable substrate using an optical tensiometer (Make: Biolin Scientific, Model: Theta Flex).

## 3. Results and discussion

First, we demonstrate that adjusting the molecular weight of the polymer constituting the continuous phase influences the stability of the emulsion droplets. By referring to Figure S1 (Please refer to Figure S1 of SI) and the tracking videos (Please refer to Supplementary Information), we draw the conclusion that the emulsion droplets stabilized by HS-40 nanoparticles in the presence of PEO labelled with a molecular weight of 1E5 destabilize catastrophically within one week of



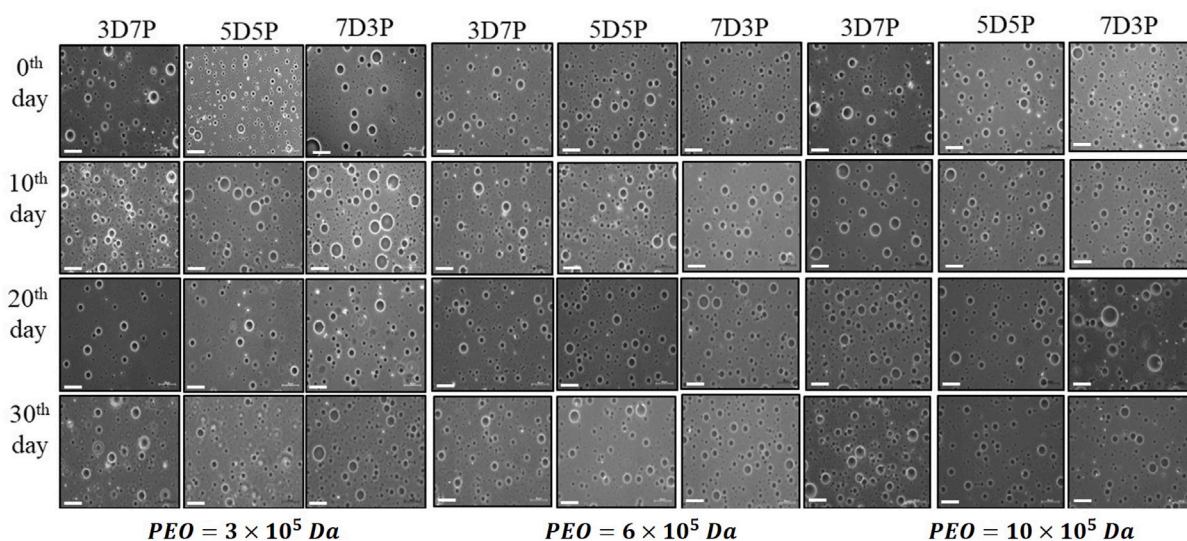


Fig. 2. Inverted microscopic images showing the structural state of w/w emulsions stabilized by HS-40 at different storage times, molecular weight of PEO, and concentration of PEO/dextran. The scale bar given in the images corresponds to 50  $\mu\text{m}$ .

sample preparation. This finding was consistent with our recent report published by our group for w/w emulsion droplets stabilized by HS-40 or CL-30 alone using a vortex mixer [4]. Compared to the vortex mixture, the stability of w/w emulsion droplets stabilized by HS-40 alone using homogenizer increased slightly, albeit the entire system remained stable for only up to seven days. Further, we looked into how the molecular weight of the polymers played a role in producing stable w/w emulsion droplets in addition to the external processing aids like an emulsifying device because, unlike o/w and w/o emulsions, w/w emulsions are primarily concerned with polymer-particle and particle-particle interactions. We envisaged that a change in molecular weight would have an impact on interactions and viscosity, preventing early droplet disintegration via coalescence.

The systematic experimental observation by adjusting polymers' concentration, molecular weight, and storage time suggests that emulsion-filled gels can be produced without heat treatment, acidification, enzyme treatment, or adding calcium ions to the formulations. The images of vials in Figure S2 (Please refer to Figure S2 of SI) illustrate the emulsion-gel transition in ATPS. The transition from emulsion to emulsion-filled gels is readily seen in the images of the vials. On day zero, the sample corresponding to 3D7P (3% dextran and 7% PEO) generated from PEO with a Mwt of  $10 \times 10^5$  Da displays emulsion gel formation. Observations made after 48 h have been used as a reference point, i.e., 0th day, for all samples. After 30 days of observation, a similar transition was detected in the 5D5P (5% dextran and 5% PEO) sample of  $10 \times 10^5$  Da. Please notice that vials 3D7P (all time points) and 5D5P (30th day), which correspond to the molecular weight  $10 \times 10^5$  Da, have been presented inverted. The gel formation was so robust that even after 90 days of observation, it did not flow when held inverted. Figure S3 shows that generating emulsion-filled gels requires a combination of high molecular weight PEO, dextran and low-concentration silica nanoparticles. However, high molecular weight PEO and low concentration silica nanoparticles alone did not create permanent gels. Several experiments have shown that when a low molecular weight component (D) is dispersed in a matrix of high molecular weight polymers, such as PEO, the inter-molecular forces between the polymer (D)-polymer (P) and polymer (P)-particles are strong enough to hold their weight. We postulate that the silica nanoparticles' strong attraction to the PEO active sites may result in the formation of an intricate three-dimensional network structure.

Fig. 2 depicts the representative inverted microscopic images of w/w emulsions stabilized by HS-40 nanoparticles. Intriguingly, the droplets produced by the emulsification have stayed stable for 30

days without transforming into a secondary state such as bijels or bi-continuous channels. We reported such a transition from droplets to bijels in ATPS stabilized by oppositely charged nanoparticles (OCNPs), which was published elsewhere [4]. Therefore, we assert that the micro-graphed structure is in a condition of thermodynamic equilibrium. Furthermore, we characterized the samples using fluorescent microscopy to probe the type of emulsion formed. We employed fluorescently-labelled dextran to visualize the structure of the emulsion state distinctly. As can be seen from Fig. 3, the continuous phase is composed of the polymer with the highest concentration. Thus, dextran-in-PEO (D/P) was seen with 3D7P, whereas 7D3P led to the phase inversion of PEO-in-dextran (P/D) independent of the PEO molecular weight employed. This trend agrees with the works of several researchers reported in the literature [22–25]. The dextran utilized in the emulsification process was fluorescently tagged with FITC. As a result, the droplets in the image become green while the PEO remains black. The investigation based on Figs. 2 and 3 aided in the development of the state diagram (Please refer to Figure S4 of SI). Figure S4 is a state diagram illustrating the phase inversion and Pickering emulsion-to-emulsion-filled gel transition under specific experimental conditions. Intriguingly, ATPS exhibits three distinct structural states as a function of Mwt, the concentration of PEO and dextran, and ageing time: (1) D/P droplets, (2) P/D droplets, and (3) D/P emulsion-filled gels.

Next, we present the stability analysis using the “creaming index (CI)”. Note: Since catastrophic breakdown occurs in the sample corresponding to PEO with a Mwt of  $1 \times 10^5$  Da, we have excluded them from the CI investigations. We chose to demonstrate the stabilization of w/w emulsion at three different two-phase system compositions, i.e., 3% dextran & 7% PEO (3D7P), 5% dextran & 5% PEO (5D5P), and 7% dextran & 3% PEO (7D3P). These combinations of PEO and dextran represent two-phase systems per the binodal curve reported by our group earlier [4]. The CI quantifies the volume fraction of emulsion generated in the binary mixture. In the production of emulsion products, a CI of 80%–100% is often considered to be substantial. For the calculation of CI, we determine the ratio of h/H based on the image analysis using ImageJ. The average value of h/H is reported by analysing several images obtained from each vial. Thus, the average CI value multiplied by 100 for each sample is plotted against the number of days to determine any divergence from the reference point (0th day). Fig. 4 describes the creaming index of the samples corresponding to  $3 \times 10^5$ ,  $6 \times 10^5$ , and  $10 \times 10^5$  Da. By referring to Fig. 4, we understand that the particle-stabilized emulsion or emulsion-filled gels remained intact regardless of the molecular weight of PEO and the compositions

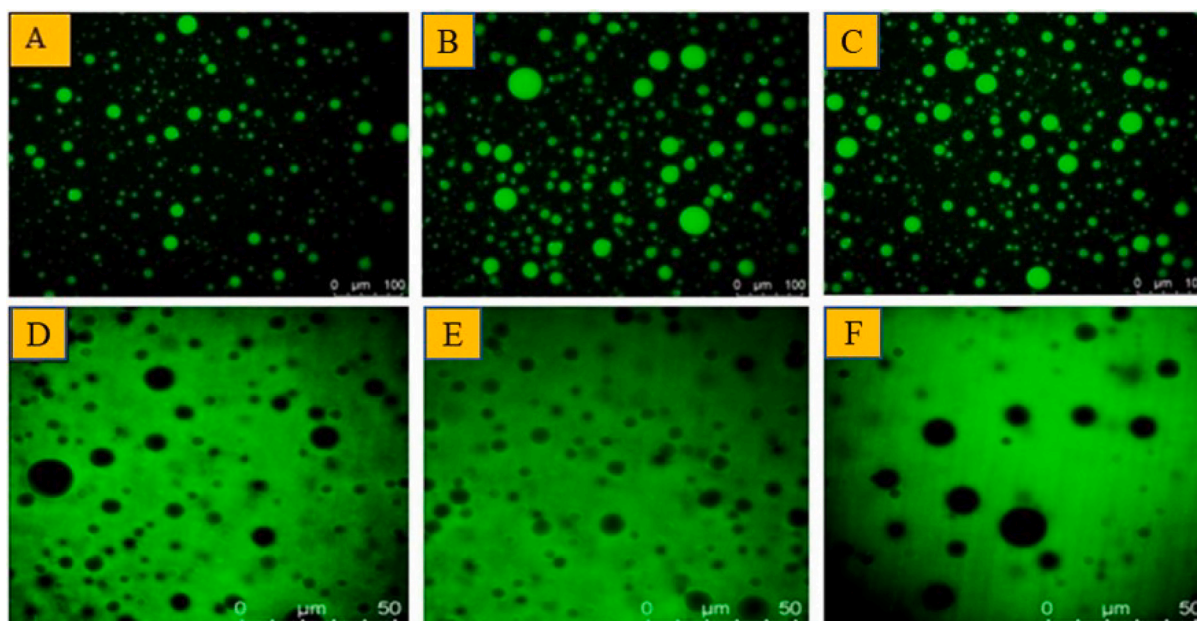


**Fig. 3.** Fluorescent microscopic images demonstrating the type of emulsions formed at a different molecular weight of PEO and the concentration of PEO/dextran. (A–C) The state of emulsion generated from the aqueous solutions of dextran and PEO with different molecular weights of  $3 \times 10^5$ ,  $6 \times 10^5$ , and  $10 \times 10^5$  Da at 3D7P, respectively. (D–F) The state of emulsion generated from the aqueous solutions of dextran and PEO with different molecular weights of  $3 \times 10^5$ ,  $6 \times 10^5$ , and  $10 \times 10^5$  Da at 7D3P, respectively.

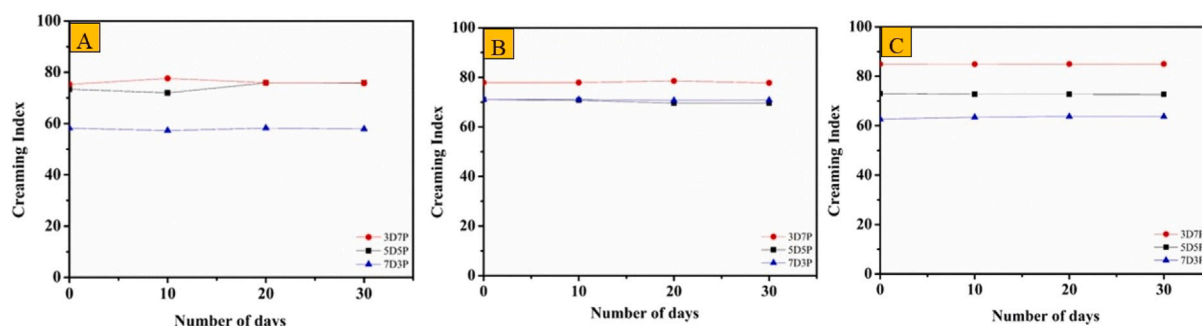


**Fig. 4.** Creaming index of ATPS pertaining to different molecular weights. (A)  $3 \times 10^5$  Da, (B)  $6 \times 10^5$  Da, and (C)  $10 \times 10^5$  Da, respectively.

of binary systems. This behaviour represents the synergistic ability of a PEO with a larger molecular weight PEO ( $> 1 \times 10^5$ ) to stabilize ATPS as a stabilizer. As a result of the synergistic action of PEO and nanoparticles, the average value of CI for the sample corresponding to  $10 \times 10^5$  Da and 3D7P exceed 80%, representing a noteworthy contribution.

By referring to Fig. 3, we conclude that the gels created in our work are not emulsion gels since there is no evidence of fractal network creation or droplet flocculation. The lack of droplet flocculation might be due to steric repulsion generated by polymer molecules grafted to the surface of silica nanoparticles. However, the transition from emulsion to emulsion-filled gels observed in the samples corresponding to  $10 \times 10^5$  Da (Please refer to Figure S2 of SI for the details) intrigued us to probe the micro-morphology of the obtained structures. We visualized the dried form of the textural features of the sample by scanning electron microscopy (SEM). The sample's microstructure corresponding to Fig. 5A depicts the gelling nature of PEO and droplets (active filler) due to the adsorption of PEO on the silica nanoparticles. In contrast, the morphology shown in Fig. 5B is analogous to the inactive filler particle arrangement, as reported by several researchers in the literature [10,18,26]. We attribute this structural arrangement of “inactive and active filler particles” to the weak interaction between PEO-dextran and dextran-particles and the strong interaction between PEO-particles. The weak interaction between particle-stabilized droplets and dextran

causes discontinuity at the junction, and therefore, the gel formed at dextran-rich compositions (7D3P) did not yield emulsion-filled gels even when PEO with a higher molecular weight ( $10 \times 10^5$ ) was employed. Consequently, the classification of the diverse ATPS samples revealed two main types of gels: (1) permanent gel and (2) weak gel. According to the state diagram in Figure S4, these permanent and weaker gels are described as particle-stabilized emulsion-filled gels and P/D or D/P emulsions. It is essential to resort to suitable structural probing as the light microscopic analysis did not aid in visualizing the emulsion-filled gel distinctly. Using a rheometer, we tested diverse ATPS samples to qualitatively and quantitatively characterize the transition.

We performed oscillatory shear tests by subjecting samples to strain and frequency sweeps. First, strain sweep tests were performed for all the samples generated with various molecular weights of the polymer at strain  $\gamma = 0.01\%$ – $100\%$  (see Fig. 6) at constant angular frequency  $\omega = 10$  rad/s and constant temperature  $25^\circ\text{C}$ . In Fig. 6, we plotted the ratio of loss to storage modulus ( $\tan(\delta) = G''/G'$ ) v/s  $\gamma$  for different times. The constant value of  $\tan(\delta)$  indicates that the linear viscoelastic zone occurred until 10% strain and that all molecular weight systems exhibited liquid-like behaviour. Further rise in shear strain  $\gamma$  results in a rapid increase in  $\tan(\delta)$ , indicating that the produced gel is deforming or droplets are elongated in the direction of the applied shear. As can be inferred from Figs. 6 A, D, and G, there is no change in the  $\tan(\delta)$  with time, which represents the usual rheological properties of emulsion



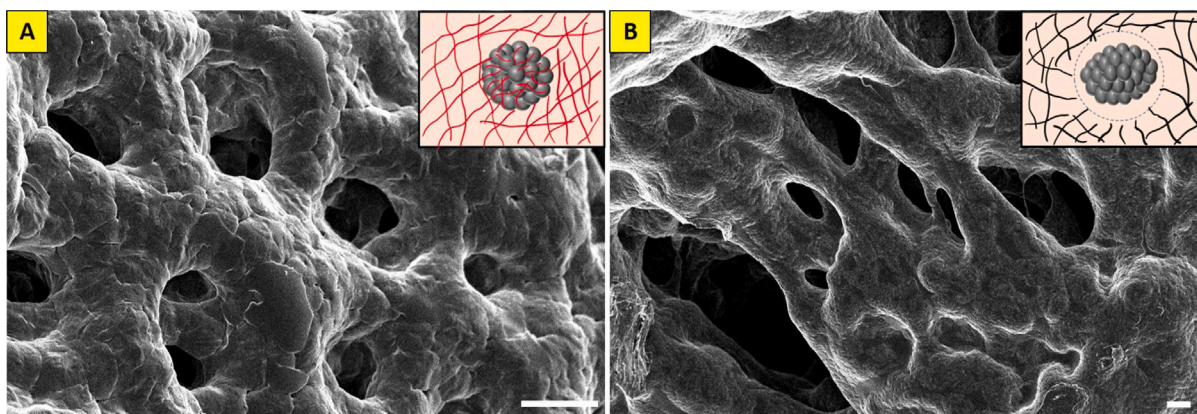


Fig. 5. The scanning electron microscopy images showing the micro-structure of  $10 \times 10^5$  Da samples at different compositions after drying. (A) 3D7P (B) 7D3P, respectively. The scale bar given in the images corresponds to 50  $\mu$ m.

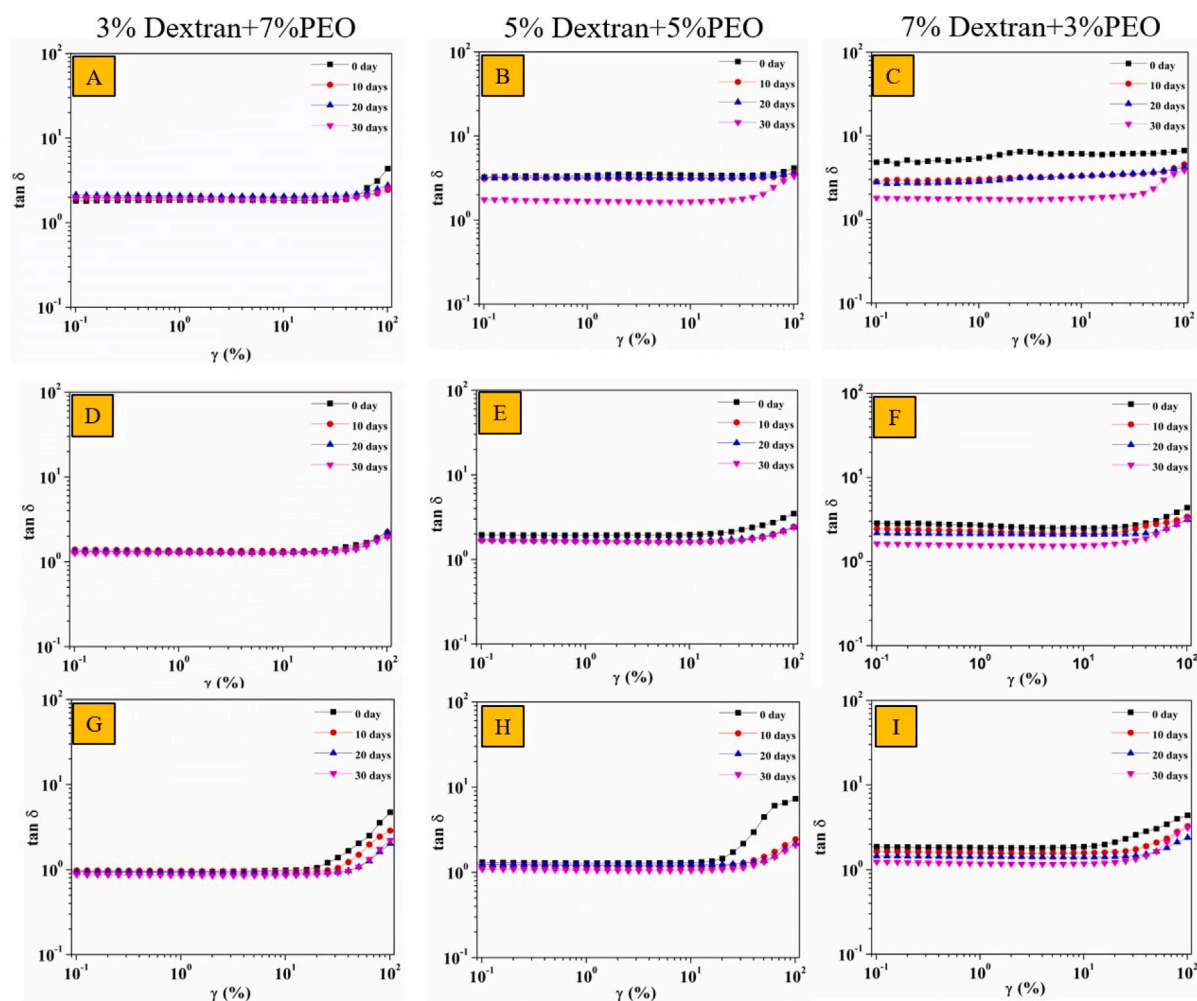


Fig. 6. Strain sweep of the formed emulsion gel. (A–C) PEO with the molecular weight of  $3 \times 10^5$  Da, (D–F) PEO with the molecular weight of  $6 \times 10^5$  Da, (G–I) PEO with the molecular weight of  $10 \times 10^5$  Da.

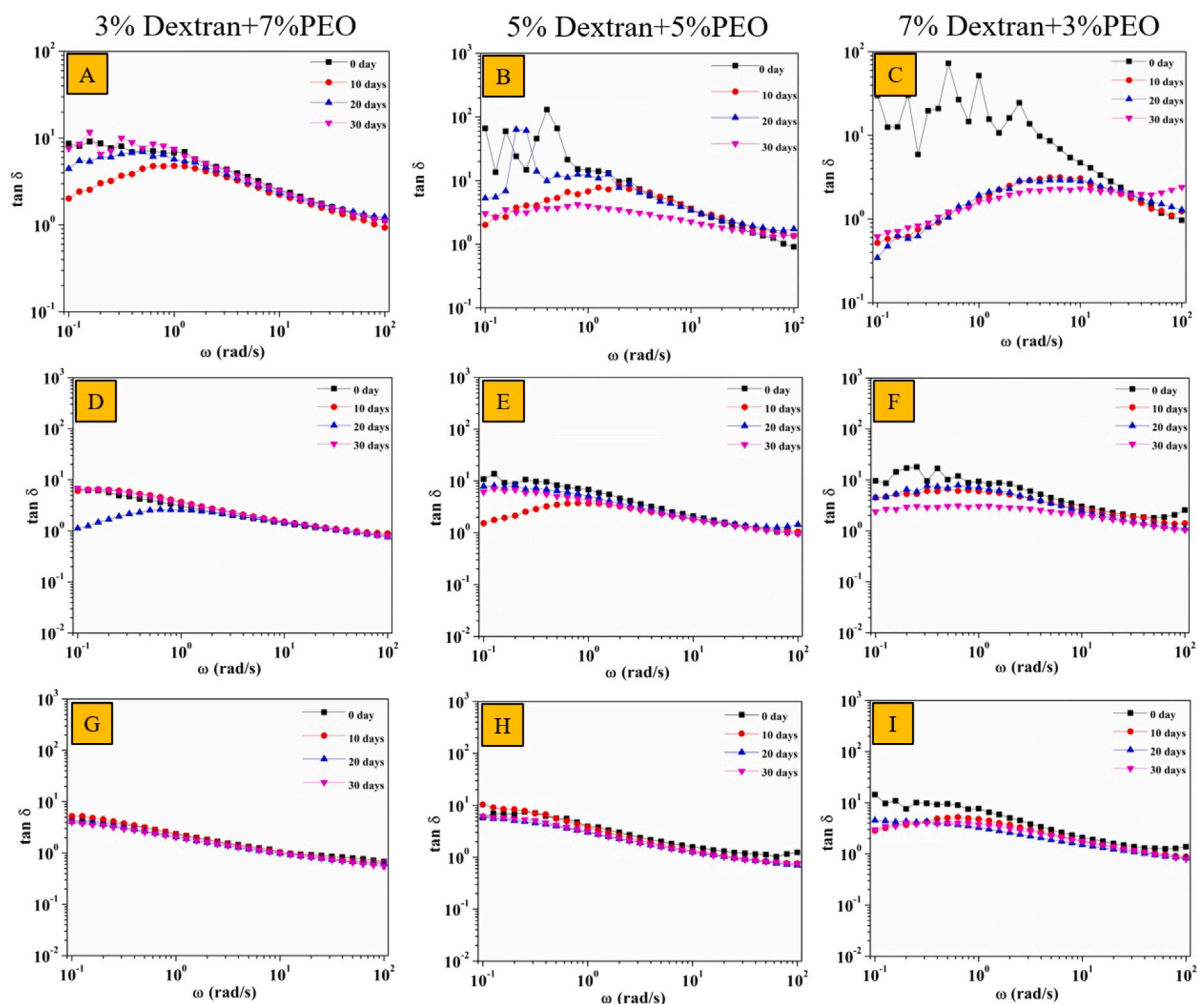


Fig. 7. Frequency sweep of the generated emulsion systems. (A–C) PEO with the molecular weight of  $3 \times 10^5$  Da, (D–F) PEO with the molecular weight of  $6 \times 10^5$  Da, (G–I) PEO with the molecular weight of  $10 \times 10^5$  Da.

systems and can be deformed when high shear is applied. On the other hand, as the concentration of non-gelling phase polymer went up, we observed a slight or significant change in  $\tan(\delta)$  over time, regardless of the molecular weight (Please refer to Figs. 6 B, C, E, F, H, and I). Changes in  $\tan(\delta)$  over time suggest that gels are forming and emulsion phases are changing because the composition of the systems is changing from 7D3P to 3D7P. We did not observe a crossover between  $G'$  and  $G''$  in the strain sweep, which suggests that the gel is like a liquid or is soft.

Experiments on frequency sweeps were conducted at a constant  $\gamma = 0.1\%$  (under linear viscoelastic region (LVE)) from  $\omega = 100 - 0.1$  rad/s at  $25^\circ\text{C}$  (Fig. 7). The produced emulsion/gel exhibits frequency-dependent behaviour in terms of molecular weight and polymer concentration. At a low molecular weight of PEO (Please refer to Figs. 7A–C) and at a higher frequency, there is no crossover of  $G'$  &  $G''$  and  $\tan(\delta)$  is almost equal to 1 for all polymer concentrations except for 7D3P at lower frequencies. In addition, the rise in  $\tan(\delta)$  with decreasing frequency indicates that there is no gel formation in the system, as it acts as a liquid. The  $\tan(\delta)$  shows maxima for all concentrations. This maximum shifts towards the higher frequency as we increase the concentration of non-gelling polymer, i.e. dextran (Fig. 7A–C). We ascribe the small reduction in  $\tan(\delta)$  for the 7D3P system below 1 to the solid-like behaviour of droplets at lower frequencies.

Further increasing the molecular weight from  $3 \times 10^5$  to  $6 \times 10^5$  Da of PEO, we did not see any gel formation until the 30th day (Please refer to Figs. 7 D–F). However, a further increase in the molecular weight

of the PEO from  $6 \times 10^5$  to  $10 \times 10^5$  Da leads to the gel formation, and hence the crossover at a frequency of  $\omega \approx 30$  rad/s is observed. For the maximum concentration of gelling polymer (3D7P), the ratio of loss to storage modulus is less than 1 ( $\tan(\delta) < 1$ ), indicating the solid-like behaviour as early as the 0th day. On day 30, gel formation is detected at a frequency of  $\omega = 80$  rad/s when the concentration of dextran is raised to 5D5P. This trend demonstrates that gel formation is a time-dependent phenomenon, implying that the adsorption of free polymer in the continuous phase is sluggish at equal polymer concentrations. We hypothesize that the change in the continuous phase composition at the end of 30 days would have caused the transition from emulsion to a gel state. In other words, the diffusion of PEO molecules from the interior of droplets to the exterior (bulk) would have helped attain the required concentration of PEO to induce gelling. All emulsions act as liquids at lower frequencies, confirming the frequency-dependent behaviour of the system.

Next, we demonstrate the viscosity of the emulsions for all compositions and molecular weights of PEO. As shown in Fig. 8, the viscosity of the emulsion was measured as a function of shear rate ( $\dot{\gamma} = 0.01 - 100 \text{ s}^{-1}$ ). Due to changes in the structure and arrangement of the droplets, the viscosity of all emulsion compositions exhibits shear-thinning behaviour at high shear rates. In all cases, the viscosity drops gradually, followed by a sudden reduction at a high shear rate. At first, confined droplets resist the shear force. Further increment in the shear rate forces the droplets to lengthen in the direction of the applied shear, resulting in a minor reduction in viscosity. After a critical shear

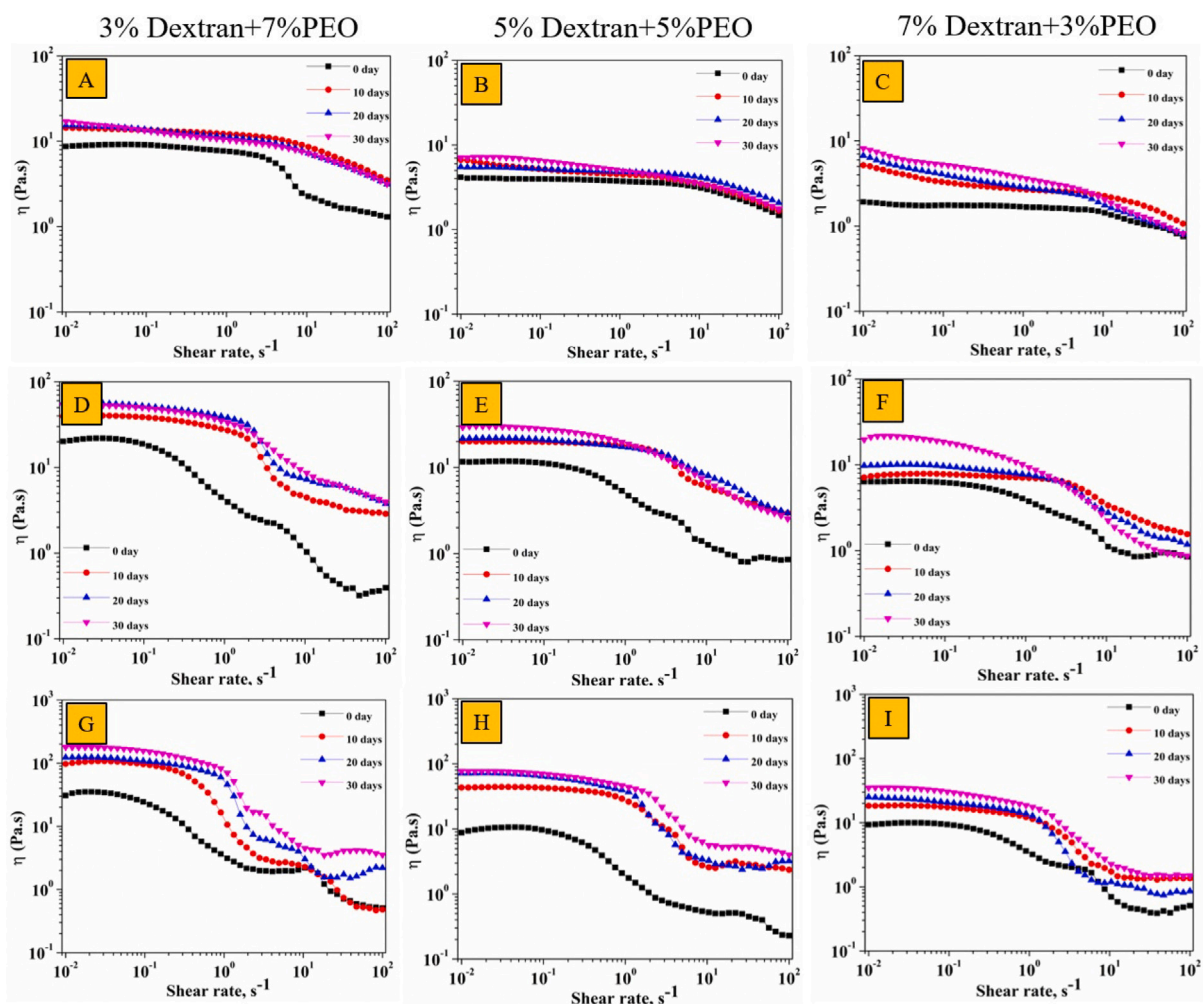


Fig. 8. Viscosity of the formed emulsion. (A–C) PEO with the molecular weight of  $3 \times 10^5$  Da, (D–F) PEO with the molecular weight of  $6 \times 10^5$  Da, (G–I) PEO with the molecular weight of  $10 \times 10^5$  Da.

rate, the elongated droplets fragment into smaller droplets, and the viscosity stabilizes after a rapid decrease. Nicolai et al. demonstrated similar phenomena of the droplet deformation under shear in w/w emulsion [27]. Increasing the molecular weight of the polymers leads to an increase in the emulsion's viscosity (Please refer to Fig. 8). As shown in Figs. 8 A–C, for the emulsion with low molecular weight PEO ( $3 \times 10^5$  Da) at a high concentration of PEO (3D7P), viscosity is high, and the droplets are stable concerning the time, while at low concentration (7D3P) the emulsion shows the low viscosity and increment with time because the trapped droplets tend to form weak network structures in non-gelling phase. This increase in viscosity with time is consistent with the gel formation findings as a function of time stated before. The emulsion with an equal concentration of both polymers (5D5P) shows the intermediate results in all the molecular weight systems. Further increasing the molecular weight (from 6 to  $10 \times 10^5$  Da) (Please refer to Figs. 8 D–F and G–I), leads to an increase in the viscosity of the system, which is in agreement with the typical characteristics of a polymer solution, i.e., higher molecular weight corresponds to a high number of polymer chains and thus the higher viscosity. By referring to Fig. 8, we infer that the droplets tend to rupture under shear, resulting in the shifting of a dramatic reduction in viscosity. This behaviour is often encountered in emulsions that undergo a phase transition. The increase in viscosity with time demonstrates the increased adsorption of the polymer on the particle-stabilized droplets.

To understand the influence of time on the emulsion and the gel, we plotted the change in storage and loss moduli at  $\gamma = 0.1\%$  and

$\omega = 10$  rad/s within the LV region and viscosity at  $\dot{\gamma} = 0.1$  s $^{-1}$ , with respect to time, as shown in Fig. 9. At low molecular weight ( $3 \times 10^5$  Da), we observed that the loss modulus is more than the storage modulus till 30 days in all compositions, which shows that there are no gel formations at the low molecular weight (Please refer to Fig. 9A). The slight increase in  $G'$  &  $G''$  is due to the droplet arrangement under the shear. The viscosity of all emulsions increases till the 10th day in all the compositions, while in 3D7P and 5D5P is constant after the 10th day as shown in Fig. 9D. Further increasing the molecular weight of the gelling phase polymer ( $6 \times 10^5$  Da) (Please refer to Fig. 9B) increases the adsorption of the polymer chain on the particles showing a significant rise in  $G'$  as compared to lower molecular weight. However, no gel formation is happening till 30 days, irrespective of the compositions. The plot of viscosity vs time for the sample corresponding to  $6 \times 10^5$  Da capitulates the similar behaviour (Please refer to Fig. 9E).

We observed the gel formation for the 3D7P sample with the maximum molecular weight ( $10 \times 10^5$  Da) of PEO (Please refer to Fig. 9C) from day zero, resulting in  $G' = G''$ . This trend shows the gel-like property up to the 30th day, indicating the maximal polymer coverage on the droplets. In the case of 5D5P, although  $G'$  &  $G''$  are slightly different, they are constant after 10th day. Intriguingly, both  $G'$  &  $G''$  exhibit a falling trend after 20 days, which may be attributable to the change in PEO concentration from 5% to 3%. Nevertheless, the magnitude of  $G'$  is  $\approx 5$  times more than the case of  $6 \times 10^5$  Da at 7D3P. On the other hand, the viscosity of the gel after the 10th day is constant but shows a slight increase on the 30th day. This constancy



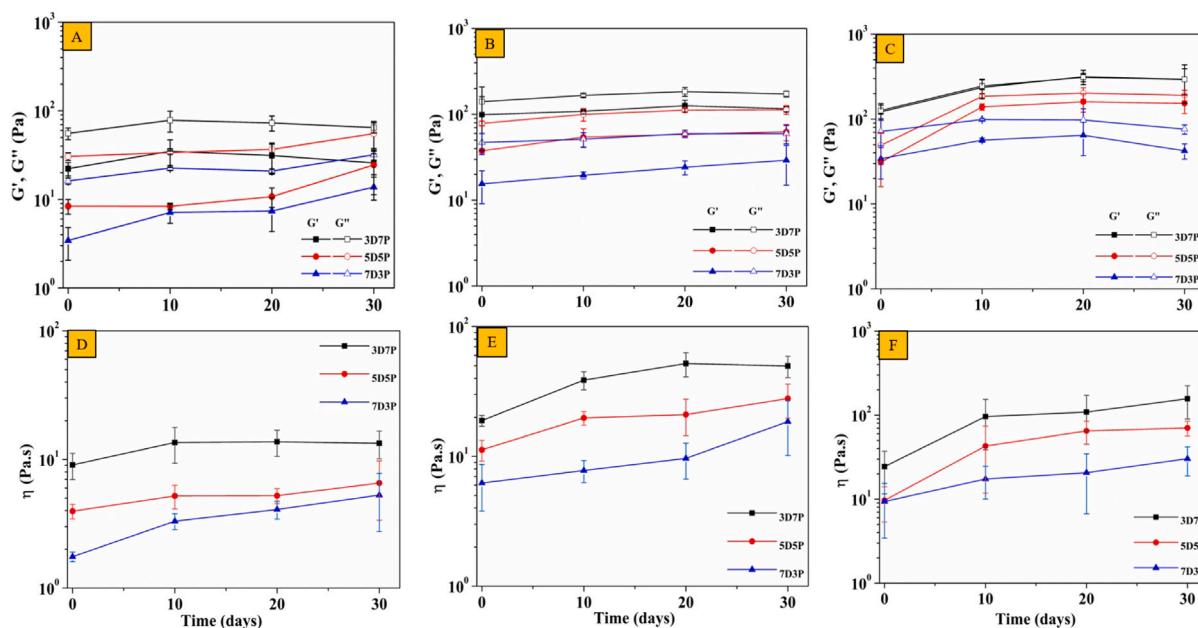


Fig. 9. Effect of storage time. (A–C) Change in storage and loss moduli of the emulsion samples prepared at a different molecular weight of PEO such as  $3 \times 10^5$ ,  $6 \times 10^5$ , and  $10 \times 10^5$  Da, respectively. (D–F) Viscosity of the emulsion samples prepared at a different molecular weight of PEO, such as  $3 \times 10^5$ ,  $6 \times 10^5$ , and  $10 \times 10^5$  Da, respectively.

in viscosity may be due to the adsorbed polymers and the arrangement of the droplets under the shear. The phase transition occurs in emulsion with composition 7D3P for all molecular weights of PEO. As shown in Fig. 9F, the viscosity of 7D3P emulsions shows a continuous increase from 0th day to 30th day which can be attributed to the gel droplets dispersed in the non-gelling polymer. These observations reiterate that the emulsion is stable up to 30th day. On a lighter side, we established the stability of the emulsions utilizing the CI investigations (Please refer to Fig. 4).

We attempted to compare the flow behaviour of emulsion and emulsion-filled gel to well-known constitutive models that typically describe the non-Newtonian behaviour of the suspensions. In 1963, I.M. Krieger presented a dimensional approach to colloidal rheology [28]. This approach is devised to apply dimensional analysis to compare the rheological behaviour of colloidal systems. The system chosen in our study is analogous to the suspension of the rigid spheres in a continuous medium. The viscosity of the model suspension proposed by I.M. Krieger depends on several factors, such as the viscosity of the medium ( $\eta_0$ ), the radius of the spheres ( $a$ ), the number density of the particles ( $n$ ), density of the particles ( $\rho_p$ ), density of the medium ( $\rho_0$ ), shear rate ( $\dot{\gamma}$ ), time ( $t$ ), and thermal energy ( $k_B T$ ). Krieger arranged these nine variables in different combinations to form six independent dimensionless groups, expressible in terms of three dimensions, to get some physical insight. Among these, the internal Reynolds number ( $R_i$ ) and colloid number ( $C$ ) best signify the motion of the colloidal spheres when exposed under different shear rates. With this insight into dimensionless groups, the rheological equation for the rigid sphere can be written as shown in Eq. (1).

$$\eta_r = f(v, C, t_r, \rho_r, R_i) \quad (1)$$

The parameters  $v$ ,  $C$ ,  $t_r$ ,  $\rho_r$ , and  $R_i$  refer to volume fraction, colloid number, reduced time, density ratio, and internal Reynolds number, respectively.

The colloid number is described as below (Eq. (2) [28])

$$C = \eta_0 a^3 \dot{\gamma} / k_B T \quad (2)$$

The parameters  $\eta_0$ ,  $a^3$ ,  $\dot{\gamma}$ ,  $k_B T$  refer to the viscosity of the medium, radius of droplets, rate of shear, and thermal energy, respectively.

The reduced viscosity ( $\eta_r$ ) is defined as follows,

$$\eta_r = \frac{\eta}{\eta_0} \quad (3)$$

Where  $\eta$  and  $\eta_0$  refer to the viscosity of the sample measured at a particular rate of shear and viscosity of the medium, respectively.

The purpose of using the Krieger constitutive relation discussed above is to compare the motion of the colloids in the emulsion as well as the gel state. The Krieger model will hold for the emulsion system as it can be treated as rigid spheres but not for the gel system, which is more complicated than a simple sphere. So, we anticipated that the samples that showed emulsion characteristics would fit the Krieger model very well. Consequently, the structural transition from emulsion to gel was distinctly seen when the molecular weight of PEO was tuned from  $3 \times 10^5$  to  $10 \times 10^5$  Da. This method helped us tell the difference between the formation of emulsion-filled gels and other structures. For brevity, we restricted our studies to higher shear rates at which the droplets would invalidate the assumptions of rigid spheres. Therefore, we performed the shear rheology with a maximum shear rate of  $100 \text{ s}^{-1}$  as the droplets exposed within this range did not elongate throughout our tests. Fig. 10 shows the model fitting on the experimental data corresponding to formed emulsion and emulsion-filled gel. The fitting of the Krieger model to the experimental data proves that the emulsion behaves like a suspension of soft polymer particles, and droplets behave like soft particles under the applied shear. Fig. 10 A and B display the characteristics behaviour of emulsion systems at 0th day and 30th day under different strain rates. We infer that there is no significant change in the rheological behaviour of the samples when compared at different storage times. Furthermore, the line drawn using the constitute relation proposed by Krieger passes through the experimental data points with no or little deviation. This trend confirms that the droplets behave like rigid particles and tend to develop robust resilience against coalescence and creaming for at least 30 days, as there was no deviation between model and experimental points on the samples corresponding to 30th day. Similar arguments can be presented for the case of  $6 \times 10^5$  Da. It is intriguing to note that the behaviour of the samples made up of  $10 \times 10^5$  Da PEO is in good agreement with the findings of other rheological studies such as frequency sweep, amplitude sweep, and a flow curve. As shown in Fig. 10 E and F, the deviation between the model and experimental

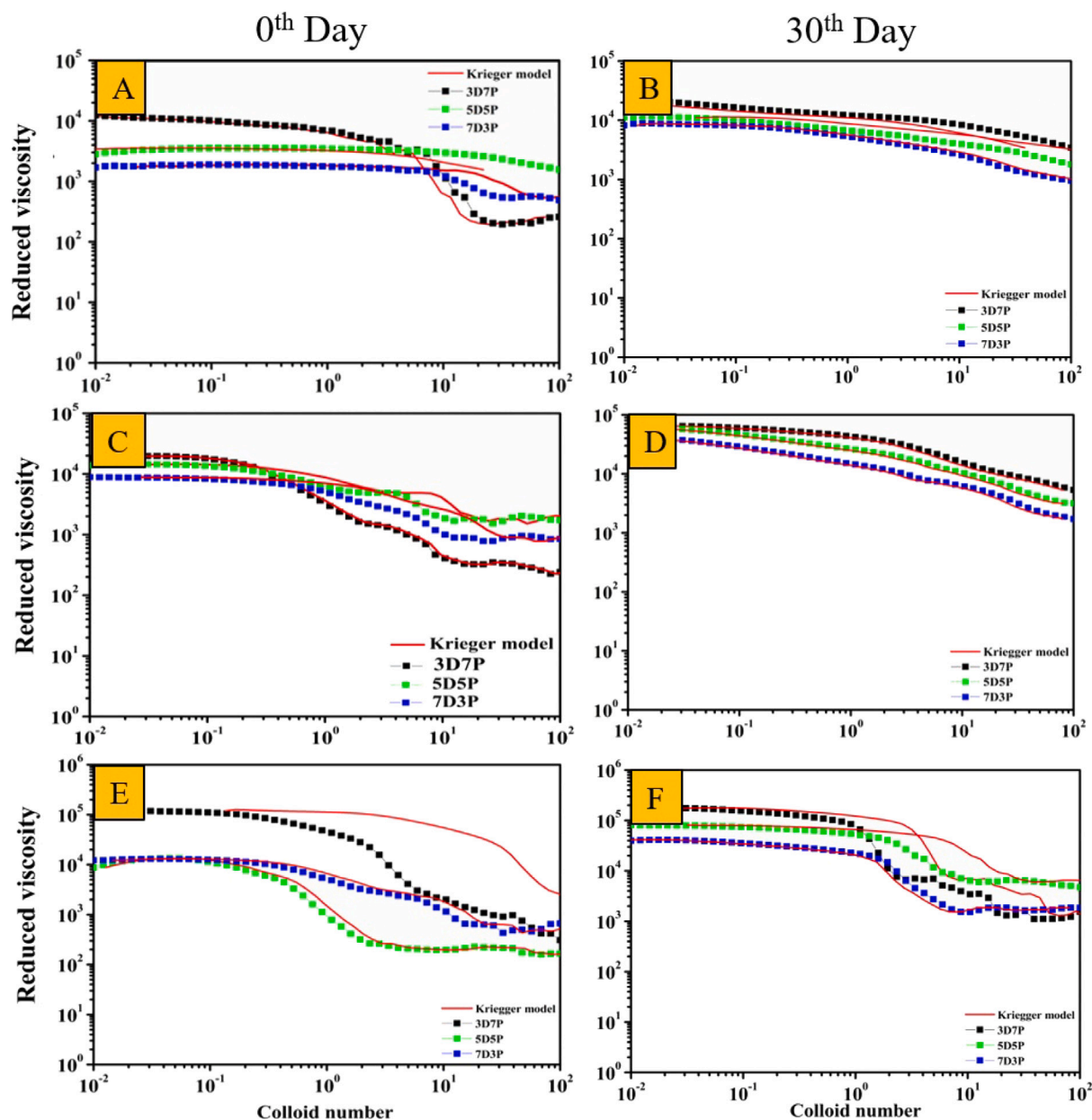


Fig. 10. Dimensional approach using Krieger model. (A, B) non-Newtonian flow curve corresponding to the PEO molecular weight of  $3 \times 10^5$  Da at 0th and 30th day, respectively. (C, D) non-Newtonian flow curve corresponding to the PEO molecular weight of  $6 \times 10^5$  Da at 0th and 30th day, respectively. (E, F) non-Newtonian flow curve corresponding to the PEO molecular weight of  $10 \times 10^5$  Da at 0th and 30th day, respectively.

data is seen. Since the sample represents the emulsion-filled gels at 0th day, the rheological behaviour corresponding to data points shown in the case of 3D7P lags behind the Krieger model to a significant level. Further, the three-dimensional network-like structure is evident from the nature of the trend that shows substantial deviation from the ideal at both 0th and 30th day for 3D7P and 5D5P, which strengthens our understanding of the occurrence of emulsion-gel transition at a particular experimental regime.

Here, we discuss the probable mechanism of structural evolution to form a three-dimensional network-like permanent gel. As discussed through the control studies (Please refer to section 3 of the Supporting Information), the combination of high molecular weight PEO, low molecular weight dextran, and a low concentration of silica nanoparticles is required to trigger the gel formation. We attribute the stability and the gel formation to the depletion flocculation induced by the adsorption of PEO on the surface of the particles. Numerous studies have discussed the nature of PEO-silica interactions, leading to the

steric (entropic) stabilization of PEO with particles in the aqueous suspensions [29–31]. To cite a few, the work of *Napper et al.* [29] and *Liu et al.* [30] present the fact about the adsorption of the poly (ethylene oxide) on silica particles due to the steric stabilization of the polymer. The rheological features of silica suspensions flocculated by a high molecular weight polyacrylamide in a given mixture were described by *Saito et al.* [31]. This study revealed that an infinite network and irreversible polymer bridging of the particles could be formed spontaneously. In 2007, *Liu et al.* studied the adsorption of PEO with different molecular weights on the surface of silica nanoparticles [32]. In that study, they reported that PEO molecules adsorb on the surface of silica nanoparticles via strong hydrogen bonding between OH groups of silica and ether oxygen groups of PEO. These authors have selected PEO with various molecular weights, including 10,000 g/mol (10E5) and 10 nm silica nanoparticles with a specific surface area of  $250 \text{ m}^2/\text{g}$ . The molecular weight and the specific surface area of interest to our study are 10E5 and  $150 \text{ m}^2/\text{g}$  (calculated), respectively. We understand

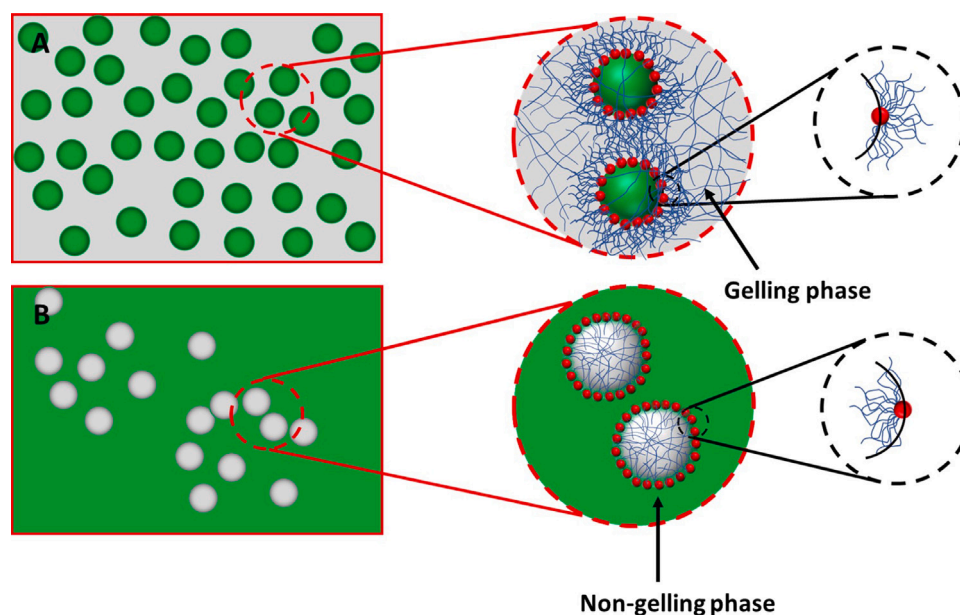


Fig. 11. Schematic illustration describing the mechanism of generating different emulsion structures depending on the type of emulsions involved, i.e., P/D or D/P. (A) Emulsion-filled gel and (B) Particle-stabilized emulsion.

from the study of Liu et al. that the zeta potential ( $\zeta$ ) decreases with an increase in molecular weight at the same concentration of PEO due to the configuration change of the PEO segments to loops [32]. The decrease in  $\zeta$  values contributes significantly to the net electrostatic attraction between the particles and polymers. The combined effect of net electrostatic attraction and flocculation (due to depletion effect) give rise to three-dimensional polymer network-like structures at a particular experimental regime, i.e., 3D7P and 5D5P at 10E5 molecular weight. Fig. 11 displays the probable mechanism of forming an emulsion-filled gel under certain conditions. As shown in Fig. 11, when the high molecular weight PEO-rich phase becomes a continuous phase, and the polymer molecules are induced to adsorb on the surface of the particles exposed to the PEO side (continuous phase), it results in the formation of particle-stabilized emulsion-filled gels instead of just w/w emulsion (Please refer to Fig. 11A). However, the opposite is true when the samples corresponding to 7D3P in ATPS undergo phase inversion, i.e., the continuous phase becomes dispersed. In this scenario, the generated droplets will behave like soft particles due to the polymer's adsorption from the droplets' interior on the surface of the nanoparticles exposed to the dispersed phase (Please refer to Fig. 11B). In short, the interactions between PEO and silica and adequate surface area drive the spontaneous formation of three-dimensional network-like emulsion-filled gels at a particular experimental regime. For instance, in the case of samples corresponding to 3D7P, the particles would maximize their contact area towards PEO being a continuous phase, as shown in Fig. 11 (A). In this case, the maximum surface exposure ensured the fast adsorption of PEO molecules on the silica particles.

Further, we conducted simple sessile drop experiments to assert the hypothesis above. The details of these experiments can be found in the Supporting Information. In short, the contact angle of water droplets containing PEO or dextran at a known concentration is determined using an optical tensiometer (Make: Biolin Scientific, Model: Theta Flex) by spreading the droplet on the modified-glass substrate. Figure S5 A shows the contact angle of an aqueous droplet containing 7% PEO established with a glass substrate modified with HS-40 nanoparticles. Please note that the glass modification is achieved by depositing a multilayer of HS-40 nanoparticles through dip coating using the procedures outlined by our group [33–35]. The contact angle of an aqueous droplet containing 3% dextran is shown in Figure S5 B. It can be inferred from Figure S5 B that the contact angle established by the aqueous dextran

droplet on the HS-40-modified glass surface is  $13 \pm 1^\circ$  (rounded off). However, since the droplet rich in PEO (7 wt%) favours the spontaneous adsorption of PEO molecules on the silica, the surface becomes modified instantly so that the system experiences pinning at the contour line. Therefore, the contact angle of the PEO droplet remained intact at  $57 \pm 1^\circ$  (rounded off) for a prolonged time. This pinning behaviour is attributed to the fast adsorption of PEO molecules on the surface of HS-40 nanoparticles [32]. A similar observation of droplet pinning with rapid adsorption of oppositely charged polyelectrolytes is reported elsewhere [36].

#### 4. Conclusion

We demonstrated a simple pathway to fabricate w/w emulsion-filled gels. These gels are permanent and remain stable against gravity for a long time. We probed the transition from emulsion-to-emulsion-filled gels using characterization techniques such as inverted light microscopy, fluorescent microscopy, and rheometer. For the first time, we show that increasing the molecular weight of the polymer that makes up the continuous phase makes the emulsion droplets more stable. This trend is because the change in molecular weight affects interactions and viscosity, which stops droplets from coming together and breaking down too quickly. Our systematic experimental findings proved that the emulsion-filled gels could be produced by adjusting the combinations of concentration, molecular weight, and storage time of the ternary systems without heat treatment, acidification, enzyme treatment or addition of calcium ions to the formulations. We employed a rheometer to characterize the particle-stabilized emulsions and emulsion-filled gels quantitatively, obtaining frequency sweep, amplitude sweep and flow curve data for the samples with different molecular weights of PEO. All rheological findings strengthen gel formation for 3D7P and 5D5P samples with the highest molecular weight ( $10 \times 10^5$  Da) of PEO. Experimental data on frequency sweep exhibited a crossover at a frequency of  $\omega = 30$  rad/s for the system with the highest concentration of PEO (3D7P), and the same has been shifted towards the right, i.e.,  $\omega = 80$  rad/s, as the concentration of PEO that constitute the continuous phase decreases (5D5P). We employed the constitutive model proposed by I.M. Krieger to describe the behaviour of emulsion and emulsion-filled gels. The model fitting on the experimental data displayed a good agreement with the Krieger model for all cases except



for the samples corresponding to  $10 \times 10^5$  Da PEO (3D7P and 5D5P compositions) at a higher shear rate. This trend captures a significant deviation from the ideal and confirms the emulsion-filled gel's state at a particular experimental regime. These gels are increasingly used in pharmaceuticals, cosmetics and food industries. Therefore, we believe the proposed study will shed some light on the characteristics of the generated emulsion-based gels and their correlation with the quality of the products.

#### Declaration of competing interest

The authors declare that they have no known competing financial interests or personal relationships that could have appeared to influence the work reported in this paper.

#### Data availability

Data will be made available on request.

#### Acknowledgements

MS acknowledges funding assistance from the Science and Engineering Research Board (SERB), India, via the SRG scheme (SRG/2019/000524). MS thanks IIT Ropar for providing a seed research grant through ISIRD (Phase 2) for setting up a laboratory.

#### Appendix A. Supplementary data

Supplementary material related to this article can be found online at <https://doi.org/10.1016/j.colsurfa.2023.131474>.

#### References

- [1] A. Maestro, J.M. Gutiérrez, E. Santamaría, C. González, Rheology of water-in-water emulsions: Caseinate-pectin and caseinate-alginate systems, *Carbohydr. Polymers* 249 (2020) 116799.
- [2] A. Florence, D. Whitehill, Some features of breakdown in water-in-oil-in-water multiple emulsions, *J. Colloid Interface Sci.* 79 (1) (1981) 243–256.
- [3] R. Hatti-Kaul, Aqueous two-phase systems, *Mol. Biol.* 19 (3) (2001) 269–277.
- [4] C. Shekhar, A. Kiran, V. Mehandia, V.R. Dugyala, M. Sabapathy, Droplet–bijel–droplet transition in aqueous two-phase systems stabilized by oppositely charged nanoparticles: A simple pathway to fabricate bijels, *Langmuir* 37 (23) (2021) 7055–7066.
- [5] G. Sala, G.A. Van Aken, M.A.C. Stuart, F. Van De Velde, Effect of droplet–matrix interactions on large deformation properties of emulsion-filled gels, *J. Texture Stud.* 38 (4) (2007) 511–535.
- [6] I.M. Geremias-Andrade, N.P. Souki, I.C. Moraes, S.C. Pinho, Rheology of emulsion-filled gels applied to the development of food materials, *Gels* 2 (3) (2016) 22.
- [7] L. Oliver, E. Scholten, G.A. van Aken, Effect of fat hardness on large deformation rheology of emulsion-filled gels, *Food Hydrocolloids* 43 (2015) 299–310.
- [8] G. Lorenzo, N. Zaritzky, A. Califano, Rheological analysis of emulsion-filled gels based on high acyl gellan gum, *Food Hydrocolloids* 30 (2) (2013) 672–680.
- [9] G. Sala, F. van de Velde, M.A.C. Stuart, G.A. van Aken, Oil droplet release from emulsion-filled gels in relation to sensory perception, *Food Hydrocolloids* 21 (5–6) (2007) 977–985.
- [10] L. Oliver, L. Berndsen, G.A. van Aken, E. Scholten, Influence of droplet clustering on the rheological properties of emulsion-filled gels, *Food Hydrocolloids* 50 (2015) 74–83.
- [11] B. Cabane, K. Wong, P. Lindner, F. Lafuma, Shear induced gelation of colloidal dispersions, *J. Rheol.* 41 (3) (1997) 531–547.
- [12] M.M. Ramos-Tejada, P.F. Luckham, Shaken but not stirred: The formation of reversible particle–polymer gels under shear, *Colloids Surf. A* 471 (2015) 164–169.
- [13] M. Kamibayashi, H. Ogura, Y. Otsubo, Shear-thickening flow of nanoparticle suspensions flocculated by polymer bridging, *J. Colloid Interface Sci.* 321 (2) (2008) 294–301.
- [14] H. Collini, M. Mohr, P. Luckham, J. Shan, A. Russell, The effects of polymer concentration, shear rate and temperature on the gelation time of aqueous silica-poly (ethylene-oxide) shake-gels, *J. Colloid Interface Sci.* 517 (2018) 1–8.
- [15] G.A. van Aken, M.H. Vingerhoeds, R.A. de Wijk, Textural perception of liquid emulsions: Role of oil content, oil viscosity and emulsion viscosity, *Food Hydrocolloids* 25 (4) (2011) 789–796, <http://dx.doi.org/10.1016/j.foodhyd.2010.09.015>.
- [16] G.A. van Aken, L. Oliver, E. Scholten, Rheological effect of particle clustering in gelled dispersions, *Food Hydrocolloids* 48 (2015) 102–109, <http://dx.doi.org/10.1016/j.foodhyd.2015.02.001>.
- [17] J. Esquena, Water-in-water (w/w) emulsions, *Curr. Opin. Colloid Interface Sci.* 25 (2016) 109–119.
- [18] E. Dickinson, Emulsion gels: The structuring of soft solids with protein-stabilized oil droplets, *Food Hydrocolloids* 28 (1) (2012) 224–241.
- [19] E. Ben Ayed, R. Cochereau, C. Dechancé, I. Capron, T. Nicolai, L. Benyahia, Water-in-water emulsion gels stabilized by cellulose nanocrystals, *Langmuir* 34 (23) (2018) 6887–6893.
- [20] L.M. Sagis, Dynamics of encapsulation and controlled release systems based on water-in-water emulsions: negligible surface rheology, *J. Phys. Chem. B* 112 (43) (2008) 13503–13508.
- [21] L.M. Sagis, Dynamics of controlled release systems based on water-in-water emulsions: a general theory, *J. Control. Release* 131 (1) (2008) 5–13.
- [22] G. Balakrishnan, T. Nicolai, L. Benyahia, D. Durand, Particles trapped at the droplet interface in water-in-water emulsions, *Langmuir* 28 (14) (2012) 5921–5926.
- [23] F. Dumas, J.-P. Benoit, P. Saulnier, E. Roger, A new method to prepare microparticles based on an aqueous two-phase system (atps), without organic solvents, *J. Colloid Interface Sci.* 599 (2021) 642–649.
- [24] A. Gonzalez-Jordan, T. Nicolai, L. Benyahia, Enhancement of the particle stabilization of water-in-water emulsions by modulating the phase preference of the particles, *J. Colloid Interface Sci.* 530 (2018) 505–510.
- [25] N. Kulkarni, E. Mani, Stabilization of water-in-water pickering emulsions by charged particles, *J. Dispers. Sci. Technol.* (2021) 1–7.
- [26] J. Chen, E. Dickinson, Effect of surface character of filler particles on rheology of heat-set whey protein emulsion gels, *Colloids Surfaces B* 12 (3–6) (1999) 373–381.
- [27] L. Tea, T. Nicolai, L. Benyahia, F. Renou, Viscosity and morphology of water-in-water emulsions: The effect of different biopolymer stabilizers, *Macromolecules* 53 (10) (2020) 3914–3922.
- [28] I.M. Krieger, A dimensional approach to colloid rheology, *Trans. Soc. Rheol.* 7 (1) (1963) 101–109.
- [29] D.H. Napper, Steric stabilization, *J. Colloid Interface Sci.* 58 (2) (1977) 390–407.
- [30] S. Liu, F. Lafuma, R. Audebert, Rheological behavior of moderately concentrated silica suspensions in the presence of adsorbed poly (ethylene oxide), *Colloid Polym. Sci.* 272 (2) (1994) 196–203.
- [31] Y. Saito, Y. Hirose, Y. Otsubo, Effect of poly (ethylene oxide) on the rheological behavior of silica suspensions, *Rheol. Acta* 50 (3) (2011) 291–301.
- [32] H. Liu, H. Xiao, Adsorption of poly (ethylene oxide) with different molecular weights on the surface of silica nanoparticles and the suspension stability, *Mater. Lett.* 62 (6–7) (2008) 870–873.
- [33] M. Sabapathy, S.D. Christdoss Pushpam, M.G. Basavaraj, E. Mani, Synthesis of single and multipatch particles by dip-coating method and self-assembly thereof, *Langmuir* 31 (4) (2015) 1255–1261.
- [34] M. Sabapathy, V. Kollabattula, M.G. Basavaraj, E. Mani, Visualization of the equilibrium position of colloidal particles at fluid–water interfaces by deposition of nanoparticles, *Nanoscale* 7 (33) (2015) 13868–13876.
- [35] M. Sabapathy, K.Z. Md, H. Kumar, S. Ramamirham, E. Mani, M.G. Basavaraj, Exploiting heteroaggregation to quantify the contact angle of charged colloids at interfaces, *Langmuir* 38 (24) (2022) 7433–7441.
- [36] M. Damak, M.N. Hyder, K.K. Varanasi, Enhancing droplet deposition through in-situ precipitation, *Nature Commun.* 7 (1) (2016) 12560.